ACS central science

Research Article

http://pubs.acs.org/journal/acscii

Human Cancer Antigen Globo H Is a Cell-Surface Ligand for Human Ribonuclease 1

Chelcie H. Eller,[†] Tzu-Yuan Chao,[†] Kiran K. Singarapu,[†,‡] Ouathek Ouerfelli,[§] Guangbin Yang,[§] John L. Markley,[†,‡] Samuel J. Danishefsky,[∥,⊥] and Ronald T. Raines*[,†,#]

[†]Department of Biochemistry, [‡]National Magnetic Resonance Facility at Madison, and [#]Department of Chemistry, University of Wisconsin—Madison, Madison, Wisconsin 53706, United States

[§]Organic Synthesis Core Facility and [∥]Laboratory for Bioorganic Chemistry, Memorial Sloan Kettering Cancer Center, New York, New York 10021, United States

[⊥]Department of Chemistry, Columbia University, New York, New York 10027, United States

Supporting Information

ABSTRACT: Pancreatic-type ribonucleases are secretory enzymes that catalyze the cleavage of RNA. Recent efforts have endowed the homologues from cow (RNase A) and human (RNase 1) with toxicity for cancer cells, leading to a clinical trial. The basis for the selective toxicity of ribonuclease variants for cancerous versus noncancerous cells has, however, been unclear. A screen for RNase A ligands in an array of mammalian cell-surface glycans revealed strong affinity for a hexasaccharide, Globo H, that is a tumor-associated antigen and the basis for a vaccine in clinical trials. The affinity of RNase A and RNase 1 for immobilized Globo H is in the low micromolar–high nanomolar range. Moreover, reducing the display of Globo H on the surface of human breast adenocarcinoma cells with a small-molecule inhibitor of biosynthesis or a monoclonal antibody antagonist decreases the toxicity of an RNase 1 variant. Finally, heteronuclear single quantum coherence (HSQC) NMR spectroscopy showed that RNase 1 interacts with Globo H by using residues that are distal from the enzymic active site. The discovery that a systemic human ribonuclease binds to a moiety displayed on human cancer cells links two clinical paradigms and suggests a mechanism for innate resistance to cancer.

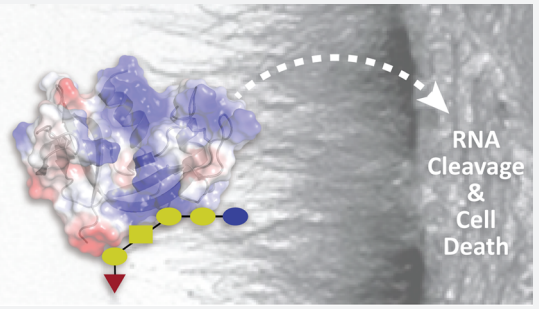

INTRODUCTION

Pancreatic-type ribonucleases (RNases) are small cationic proteins that are secreted by vertebrate cells.[1] RNase A, a renowned enzyme from cows, and RNase 1, its most prevalent human homologue, are highly efficient catalysts of RNA cleavage.[2] Moreover, when engineered to evade the cytosolic ribonuclease inhibitor protein (RI[3]), both RNase A and RNase 1 are endowed with cytotoxicity.[4−8] The putative mechanism for this cytotoxicity involves internalization of an RNase via endosomes, translocation into the cytosol, and cleavage of cellular RNA, which leads to apoptosis.[9]

Surprisingly, the cytotoxic activity of RI-evasive RNases is specific for cancer cells, and a variant of RNase 1 is undergoing clinical trials as a cancer chemotherapeutic agent.[10] The basis for the specificity of RI-evasive variants for cancerous versus noncancerous cells has been unclear. Both normal and cancerous cells contain RI at similar levels.[11] Thus, RI evasion is unlikely to play a major role in specific toxicity for cancer cells.

The surface of cancer cells is more anionic than that of noncancerous cells due to increases in glycosaminoglycan profile, phospholipid composition, and glycosphingolipid exposure.[12] In addition, cancer cells undergo constitutive endocytosis more rapidly than do matched noncancerous cells.[13] These two factors could enhance the cellular uptake of RNases.[13,14] Indeed, reducing the negative charge on a cell surface by diminishing the biosynthesis of heparan sulfate and chondroitin sulfate decreases net internalization, as does decreasing the positive charge of an RNase.[15,16] These data provide some basis for the preferential susceptibility of cancer cells to RNase-mediated cytotoxicity. Still, we suspected that other factors were likely to contribute.

Eukaryotic cells are covered by a glycocalyx: an extensive network of polysaccharides.[17] The glycocalyx serves as a rich source of binding sites for receptors and ligands, as well as pathogens and toxins. The mammalian glycome is estimated to consist of a few hundred unique glycan structures on glycoproteins and glycolipids.[18] One such glycan is Globo H.

Globo H is a neutral hexasaccharide glycosphingolipid. As a component of a glycolipid or glycoprotein, Globo H is located endogenously on the outer membrane of epithelial cells from mammary, uterine, pancreas, and kidney tissues.[19,20] Importantly, immunohistological analyses have detected high levels of

Received: April 21, 2015
Published: July 13, 2015

DOI: 10.1021/acscentsci.5b00164
ACS Cent. Sci. 2015, 1, 181−190

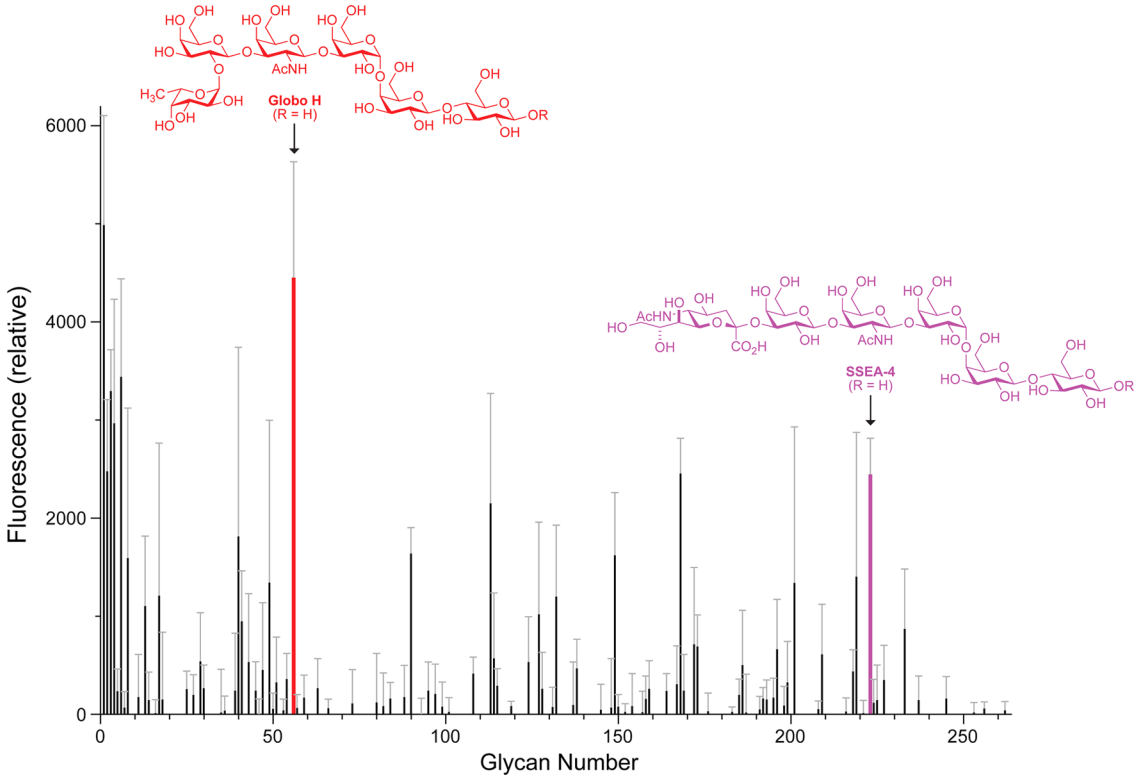

Figure 1. Histogram of the binding of RNase A to a printed array of mammalian cell-surface glycans. The array had 264 synthetic and natural amine-functionalized glycoconjugates immobilized on *N*-hydroxysuccinimide-activated glass slides.[62] In the synthesis of the glycan array, R = $(CH_2)_5NH_2$ for Globo H and R = $(CH_2)_2NH_2$ for SSEA-4. Binding was detected by fluorescence using α-RNase A and a fluorescently labeled secondary antibody. Glycans are listed in Table S1.

Table 1. Prominent Ligands for RNase A in Mammalian Glycan Array

glycan type		glycan	glycan modification
anionic glycoprotein	**1**–**3**	human α_1-acid glycoprotein	di-, tri-, tetraantennary sialylated
anionic glycoprotein	**4**	ceruloplasmin	bitriantennary *N*-glycosidic
anionic glycoprotein	**6**	transferrin	two disialylated biantennary
unbranched glycan	**56**	Globo H	Fucα1−2Galβ1−3GalNAcβ1−3Galα1−4Galβ1−4Glc
unbranched glycan	**90**		GalNAcβ1−3Galα1−4Galβ1−4GlcNAc
unbranched glycan	**223**	SSEA-4	Neu5Acα2−3Galβ1−3GalNAcβ1−3Galα1−4Galβ1−4Glc

Globo H on the outer membrane of tumor specimens from small-cell lung, breast, prostate, lung, pancreas, gastric, ovarian, and endometrial tissues.[21] Moreover, high levels of this tumor-associated antigen correlate to a poor prognosis.[22,23] Globo H could enable cancer cells to escape from immune surveillance,[24] and its intracellular binding to translin-associated factor X (TRAX) promotes angiogenesis,[25] which plays a critical role in the growth and spread of cancer. For these reasons and because its endogenous expression resides in tissues that are relatively inaccessible to the immune system, Globo H has become an attractive vaccine target for epithelial tumors.[26] This approach has been validated by the results of clinical trials in which treatment of cancer patients with up to 16 mg of a high-affinity, high-specificity[27] monoclonal antibody against Globo H (MBr1) resulted in no organ toxicity.[28] Accordingly, vaccines based on synthetic Globo H are advancing in clinical trials worldwide.[26,29−33] Despite the current therapeutic interest in Globo H, little is known about its functional role.

Here we screen a printed array of mammalian cell-surface glycans and discover that RNase A binds to Globo H. We measure the affinity of bovine RNase A and its human homologue, RNase 1, for Globo H in vitro using surface-binding assays. Then, using two distinct types of antagonists, we show that breast adenocarcinoma cells that display less Globo H are less vulnerable to cytotoxic RNases. Finally, we use heteronuclear single quantum coherence (HSQC) NMR spectroscopy to identify those residues in RNase 1 that interact with Globo H. Together, these data suggest that the interaction of RNase 1 and Globo H could underlie a previously unknown endogenous anticancer activity in humans and provide a molecular basis for the efficacy of RNase 1 variants as cancer chemotherapeutic agents.

RESULTS

Glycan Array Screening. A printed array of 264 mammalian cell-surface glycans (Table S1) was screened for ligands for RNase A. Several glycan ligands were discovered by this screen (Figure 1), and those fall into two categories: glycoproteins and unbranched glycans (Table 1). The glycoproteins bound by RNase A are serum proteins with complex glycan modifications. Human α_1-acid glycoprotein (glycans **1**−**3**) contains various forms of di-, tri-, and

DOI: 10.1021/acscentsci.5b00164
ACS Cent. Sci. 2015, 1, 181−190

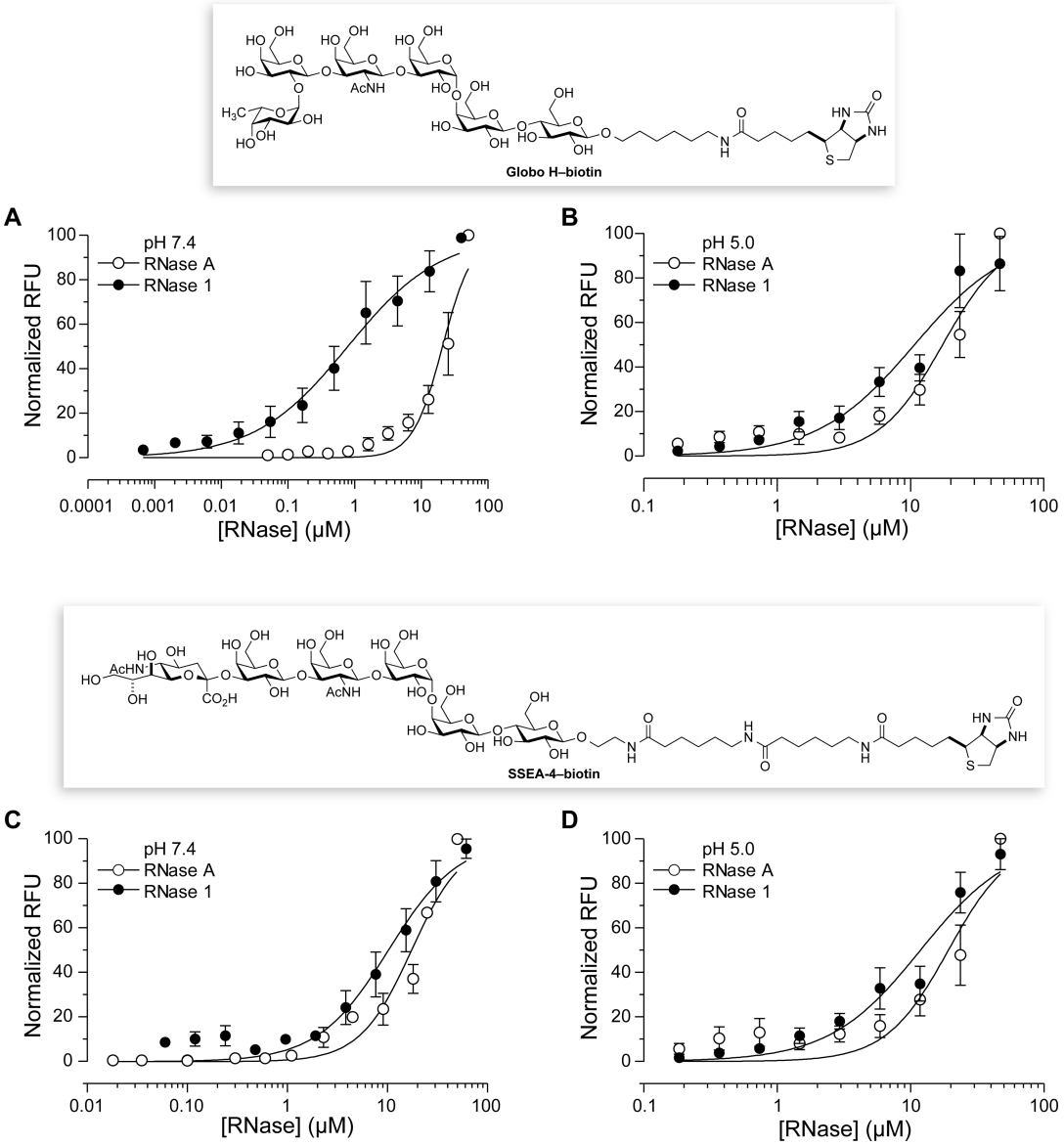

Figure 2. Isotherms for the binding of RNase A and RNase 1 to surface-bound Globo H and SSEA-4. Biotinylated glycans were immobilized on a neutravidin plate and incubated with varying concentrations of RNase–BODIPY conjugates in (A) PBS, pH 7.4, containing Tween X-100 (0.005% v/v), or (B) 20 mM Tris–HCl buffer, pH 5.0, containing NaCl (130 mM). Fluorescence emission data were fitted by nonlinear regression to eq 2. Values of K_d are listed in Table 2.

tetraantennary sialylated carbohydrate chains; ceruloplasmin (glycan **4**) possesses bi- and triantennary *N*-glycosidic glycans; and transferrin (glycan **6**) contains two disialylated biantennary glycans.[34−36] Each of these glycoproteins is anionic (p*I* 2.7−5.5). Thus, their interaction with RNase A (p*I* 9.3) could arise largely through nonspecific Coulombic interactions.

Several tetrasaccharides and hexasaccharides were also recognized by RNase A. Most prominent in the profile are the hexasaccharides Fucα1−2Galβ1−3GalNAcβ1−3Galα1−4Galβ1−4Glc (glycan **56**) and Neu5Acα2−3Galβ1−3GalNAcβ1−3Galα1−4Galβ1−4Glc (glycan **223**), both of which belong to the globo series of glycosphingolipids.[37,38] Glycan **56** is Globo H. Glycan **223** is the stage-specific embryonic antigen-4, SSEA-4, which is expressed briefly during early stages of development and in certain teratocarcinoma cells.[39,40] Surprisingly, RNase A appeared to have little affinity for the pentasaccharide precursor to these molecules, Galβ1−3GalNAcβ1−3Galα1−4Galβ1−4Glc (glycan **127**), but did bind to a similar structure, GalNAcβ1−3Galα1−4Galβ1−4GlcNAc (glycan **90**). Together, these results suggest that RNase A recognizes the core tetrasaccharide GalNAcβ1−3Galα1−4Galβ1−4Glc that constitutes all globo-series glycosphingolipids.[37,38]

Binding of RNases to Immobilized Globo H. To characterize the affinity of RNases for Globo H (glycan **56**), we used an assay that displays the glycan on a surface. Specifically, glycan−biotin conjugates were immobilized on avidin plates and incubated with various concentrations of fluorophore-labeled RNases. We found that the RNase 1·Globo H complex has $K_d = (0.8 \pm 0.2)$ μM (Figure 2A; Table 2). The affinity of RNase A for Globo H was detectable but significantly weaker, consistent with the lower abundance of this particular glycan in cows (vide infra). We likewise assessed the affinity of RNase A and RNase 1 for immobilized SSEA-4 (glycan **223**).

DOI: 10.1021/acscentsci.5b00164
ACS Cent. Sci. 2015, 1, 181−190

Table 2. Affinity of RNase A and RNase 1 for Surface-Bound Globo H and SSEA-4

		K_d[a] (μM)	
glycan	pH	RNase A	RNase 1
Globo H	7.4	21 ± 2	0.8 ± 0.2
Globo H	5.0	17 ± 2	11 ± 2
SSEA-4	7.4	17 ± 1	10 ± 1
SSEA-4	5.0	19 ± 1	12 ± 2

[a]Values (±SE) were obtained by fitting the data in Figure 2 to eq 2.

This glycan shares a pentasaccharide unit with Globo H but appeared to have less affinity for RNase A in the glycan array (Figure 1). We found that RNases did indeed bind more weakly to SSEA-4 than to Globo H (Figure 2C; Table 2).

Effect of Globo H on RNase-mediated Cytotoxicity. Globo H has been detected inconsistently in mammals. For example, this glycan is more abundant in tissues from rat than in those from cats and dogs.[41] Analyses of the globo-series glycolipids have not, however, been performed in bovine tissues. Because RNase A is derived from a cow, we probed cells from bovine mammary gland epithelial line MAC-T[42] for three globo-series glycans: Globo H, SSEA-4, and SSEA-3. Using monoclonal antibodies that are specific for these glycans,[27] a fluorescently labeled secondary antibody, and confocal microscopy, we were unable to detect any of these glycans on the surface of MAC-T cells (data not shown). Accordingly, we performed subsequent analyses with human cells.

Variants of RNase A and RNase 1 that evade cytosolic RI are selectively toxic to human cancer cells. For example, variants of RNase 1 (R39D/N67R/N88R/G89R/R91D, or "DRRRD") and RNase A (G88R) demonstrate cytotoxicity against human leukemia cells with IC_{50} values of 10.8 and 6.2 μM, respectively.[6,15] Hence, we sought to determine the effect of reducing cell-surface Globo H on RNase-mediated cytotoxicity.

Small-molecule inhibitors of glycosyltransferases can be used to modulate the display of glycans on the cell surface.[43,44] For example, 2-fluoro-2-deoxyfucose (2FF) inhibits fucosyltransferases.[43] Of the 20 highest scoring ligands in our screen (Table S2), only Globo H has a fucose unit. Intracellular esterases

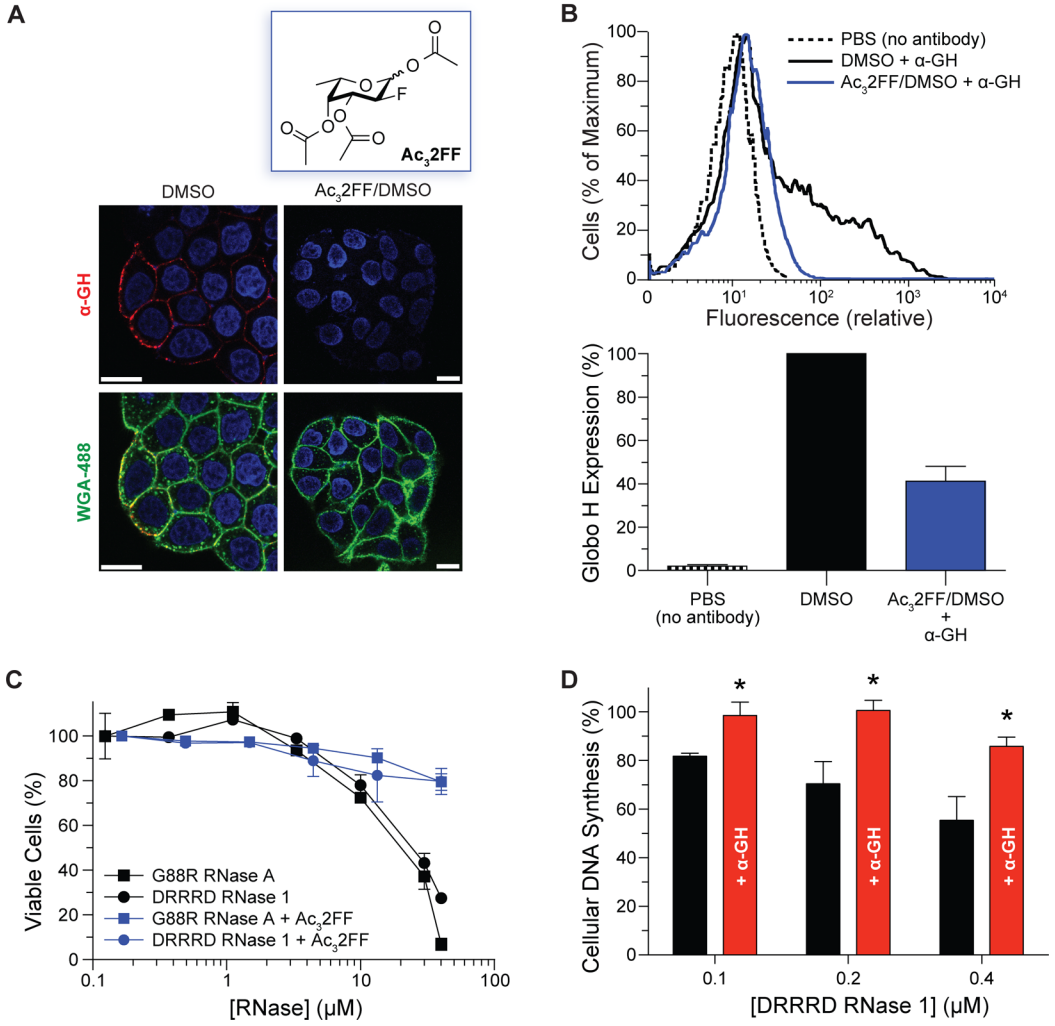

Figure 3. Effects of Globo H display on RNase-mediated toxicity for human breast adenocarcinoma cells (MCF-7). (A) Confocal microscopy to visualize the effect of $Ac_3$2FF (100 μM in 0.1% v/v DMSO) on Globo H expression. Nucleus: Hoechst 33342 (blue). α-GH: Alexa Fluor-594 (red). Outer membrane: WGA-488 (green). Scale bar: 5 μm. (B) Flow cytometry to quantify the effect of $Ac_3$2FF (100 μM in 0.1% v/v DMSO) on Globo H expression. (C) Cell viability assay to reveal the effect of diminished Globo H expression due to $Ac_3$2FF (100 μM in 0.1% v/v DMSO) on Globo H expression on the susceptibility of cells to cytotoxic variants of RNase 1 (DRRRD) and RNase A (G88R), n = 3. (D) Cellular DNA synthesis assay to reveal the effect of blocking Globo H with α-GH (15 ng/mL) on the susceptibility of cells to a cytotoxic variant of RNase 1, n = 3. *, $p < 0.01$.

DOI: 10.1021/acscentsci.5b00164
ACS Cent. Sci. 2015, 1, 181−190

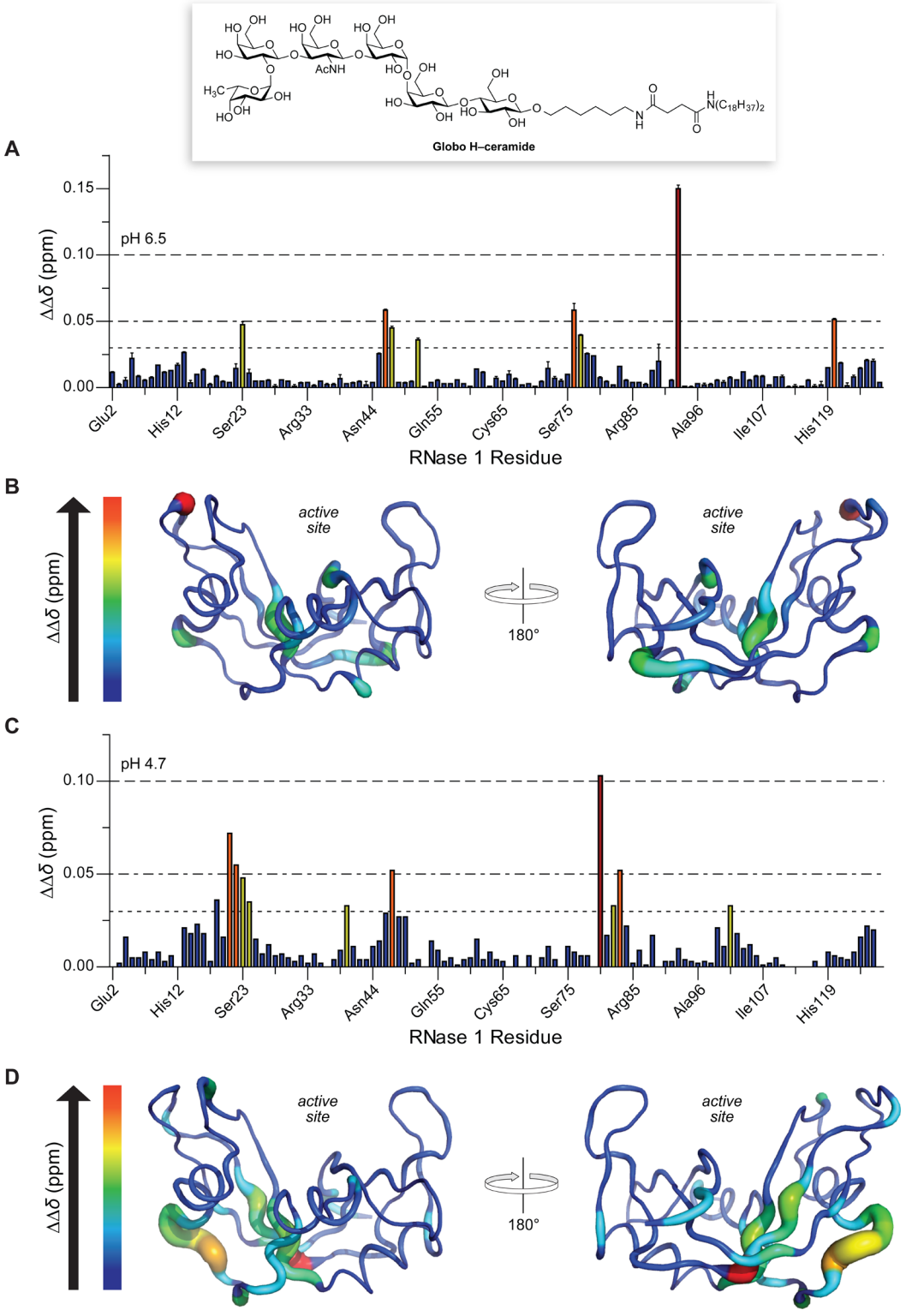

Figure 4. Solution structure of the RNase 1−Globo H interface. (A, B) pH 6.5; (C, D) pH 4.7. A solution of [^{15}N]-RNase 1 was prepared in the presence and absence of Globo H−ceramide micelles. NMR chemical shift changes ($\Delta\Delta\delta$ ppm) were calculated as the average of $n = 2$ from the vector change upon addition of Globo H−ceramide and plotted by residue (panels A and C). Changes in chemical shift are displayed with the program PyMOL (panels B and D). Backbone regions that are colored in red and that are wider indicate greater chemical shift perturbations. Raw ^{1}H,^{15}N-HSQC NMR spectra are shown in Figure S3.

convert peracetylated 2-fluoro-2-deoxyfucose ($Ac_3$2FF) into 2FF.[43] We synthesized $Ac_3$2FF and used confocal microscopy and flow cytometry to demonstrate that treating MCF-7 cells with $Ac_3$2FF reduces the surface-display of Globo H (Figure 3A and 3B). Using an assay that measures viable cells, we found that cells with lower Globo H levels were less vulnerable to cytotoxic RNase variants (Figure 3C). Finally, we used a highly sensitive assay of cellular DNA synthesis to demonstrate that α-

DOI: 10.1021/acscentsci.5b00164
ACS Cent. Sci. 2015, 1, 181−190

GH antagonizes the cytotoxicity of DRRRD RNase 1 (Figure 3D).

Globo H Binding Site on RNase 1. To identify the residues in RNase 1 that interact with Globo H, we employed $^{1}H,^{15}N$-HSQC NMR spectroscopy. The backbone chemical shifts of RNase 1 exhibited few changes in the presence of zwitterionic CTAB micelles. In contrast, these shifts were perturbed markedly by micelles containing a Globo H−lipid conjugate at 1 equiv relative to RNase 1 (Figures S3A and S3B). These changes in the vector of the chemical shift were calculated with eq 3 and plotted by residue number (Figure 4).

At pH 6.5, major shift perturbations were found throughout the amino acid sequence, being greatest at residues Ser23, Phe46, Val47, Val52, Asn76, Ser77, Tyr92, and Phe120 (Figure 4A). These perturbations were mapped onto the structure of RNase 1 to depict those regions that contribute most to the binding of Globo H (Figure 4B). The perturbations at pH 6.5 were dispersed along the protein, residing mainly in turns and bends (Table 3).

Table 3. Residues of RNase 1 That Interact with Globo H at pH 6.5

$\Delta\Delta\delta$ (ppm)	residue	structure[a]
>0.100	Tyr92	t
0.05−0.10	Phe46, Asn76, Phe120	s, b, b
0.03−0.05	Ser23, Val47, Val52, Ser77	b, s, h, b

[a]t, turn; b, bend; s, β-strand; h, α-helix.

RNase 1 undergoes endocytosis, and glycosylaminogylcans reside on the lumen of endosomes.[45] Accordingly, we also used $^{1}H,^{15}N$-HSQC NMR spectroscopy to monitor chemical shift perturbations at pH 4.7, which is encountered in endosomes.[46,47] Interestingly, we found that the larger overall shift perturbations clustered predominantly to a more polar serine-rich loop, Ser18−Thr24, as well as at His80 (Figures 4C and 4D; Table 4). As these residues are predominantly polar, the interactions are likely due to hydrogen bonding. These data suggest that the site on RNase 1 that interacts with Globo H is smaller at low pH, and that some of the multivalency that confers tighter binding is lost. These structural data are consistent with the weak affinity of RNase 1 for Globo H at low pH (Figure 2B).

Table 4. Residues of RNase 1 That Interact with Globo H at pH 4.7

$\Delta\Delta\delta$ (ppm)	residue	structure[a]
>0.100	His80	s
0.05−0.10	Ser18, Ser21, Ser22, Ser23	−, −, −, b
0.03−0.05	Thr24, Arg39, Val47, Thr82 Asp83, Lys102	b, b, s, s, s, s

[a]t, turn; b, bend; s, β-strand, h, α-helix; −, no structure.

We also used $^{1}H,^{15}N$-HSQC NMR spectroscopy to identify the residues in RNase A that interact with Globo H at pH 4.7. We found that few residues were altered (Figures S3C and S4), consistent with the weak affinity observed with binding assays (Figure 2B).

DISCUSSION

We have discovered that a protein and a carbohydrate conspire to direct the degradation of RNA within cancer cells. Specifically, we found that the major secretory ribonuclease in humans, RNase 1, interacts with a human cell-surface glycan, Globo H, which is a tumor-associated antigen (Figure 1). The affinity of RNase 1 for this neutral glycan is in the high nanomolar range at physiological pH (Figure 2A; Table 2). As both RNase 1 and Globo H are the basis for ongoing clinical trials,[10,33] our discovery links two molecules that are now in the clinic. Moreover, our discovery rationalizes the selective cytotoxicity of RNase 1 variants for cancerous versus noncancerous cells while revealing an endogenous ligand for Globo H.

RNases are known to interact with anionic cell-surface glycans. Indeed, sialic acid and heparan sulfate play a role in the cellular uptake of RNases.[2,16] These interactions are manifested primarily through nonspecific Coulombic interactions with cationic side chains of RNases. While evidence mounts that RNase 1 degrades extracellular RNA and, thus, regulates hemostasis and immunity,[2,48] no specific cell-surface ligand for RNase 1 is known.

Globo H is a specific ligand for RNase 1. An RNase−Globo H interaction was apparent regardless of whether the glycan was displayed on a slide (Figure 1), in the well of a plate (Figure 2), or on a micelle (Figure 4). As these three display modes have only Globo H itself in common, their readout validates Globo H as a ligand for RNase 1. Moreover, reducing the display of Globo H on the surface of breast adenocarcinoma cells by two distinct methods (i.e., a small-molecule inhibitor of biosynthesis or a monoclonal antibody antagonist) makes cells less susceptible to a cytotoxic variant of RNase 1 (Figure 3). We note that cell-surface components change during tumorigenesis,[12] and such changes could amplify selective toxicity that is based on the differential display of Globo H.

RNase A and RNase 1 have 82% identity in their amino acid sequence. Correspondingly, the two enzymes appear to interact with Globo H in a similar manner, albeit with different affinity (Table 2). Of the eight residues of RNase 1 that were perturbed most upon binding to Globo H at neutral pH, six are conserved in RNase A. Only Val52 and Asn76, which are alanine and tyrosine residues in RNase A, differ. Eight of 11 residues of RNase 1 that were perturbed most upon binding at low pH are in RNase A, with Thr24, His80, and Lys102 of RNase 1 being replaced with serine, asparagine, and alanine, respectively, in RNase A.

Like Globo H, glycosaminoglycans reside on the surface of human cells. Sulfated glycosaminoglycans are known to bind to RNase 1, presumably via favorable Coulombic interactions with the cationic active site.[2,14,16,49] The residues that interact with Globo H are distal from the enzymic active site (Figures 4B and 4D). Accordingly, RNase 1 could employ multivalency in its binding to human cells. This mode of binding is consistent with an experimental/computational study that concluded that specific (though unidentified) cell-surface components and nonspecific Coulombic interactions both contribute to the cellular uptake of RNase 1.[14]

Along with other cell-surface glycans,[45] Globo H is likely displayed on the interior of endosomes following endocytosis. Interestingly, NMR analyses reveal that the binding sites on RNase 1 for Globo H differ with pH (Figure 4). At acidic pH, these sites cluster and become weaker. These data, which are consistent with observed values of K_d (Figures 2A and 2B; Table 2), suggest a mechanism in which RNase 1 is released from lumenal Globo H as endosomes mature, allowing for the entry of RNase 1 into the cytosol.

DOI: 10.1021/acscentsci.5b00164
ACS Cent. Sci. 2015, 1, 181−190

Interestingly, other RNase ligands in the glycan array include sialic acid glycoproteins (Figure 1 and Table 1). These proteins include the transporter, α_1-glycoprotein, whose role is largely unknown aside from being a carrier that can improve the pharmacokinetics of small-molecule drugs.[50] Ceruloplasmin is a copper-binding protein that associates with transferrin, an iron-binding protein. An interaction with these proteins could enable an unmodified enzyme to avoid renal filtration in vivo. This mechanism could be more advantageous than PEGylation, which increases the circulation time of RNases in mice but at the expense of cellular uptake and enzymatic activity.[51,52]

For over 50 years, thoughts about pancreatic-type ribonucleases have been dominated by RNase A. This renowned enzyme has been the basis for much seminal work in biological chemistry, resulting in the first enzymatic reaction mechanism[53,54] along with four Nobel prizes.[55−57] New work has, however, revealed substantial differences in the biochemical and biological properties of RNase A and its human homologue, RNase 1.[2] We have discovered another difference, and propose that affinity of RNase 1 for Globo H evolved for a specific purpose: to defend the host organism against cancer.

METHODS

Materials. MCF-7 cells were from ATCC (Manassas, VA). Phosphate-buffered saline (PBS) (Ca^{2+}- and Mg^{2+}-free), Dulbecco's modified Eagle's medium (DMEM), and fetal bovine serum (FBS) were from Life Technologies (Grand Island, NY).

A rabbit polyclonal IgG antibody to RNase A (α-RNase A) was from Biodesign International (Kennebunk, ME); a secondary goat α-rabbit IgG−Alexa Fluor 594 conjugate was from Invitrogen (Carlsbad, CA). A murine monoclonal IgM antibody to Globo H (MBr1 or α-GH) was from Enzo (Farmingdale, NY); secondary goat α-mouse IgG−Alexa Fluor 594 and IgG−Alexa Fluor 647 conjugates were from Life Technologies.

[^{15}N]-NH_4Cl was from Cambridge Isotope Laboratories (Andover, MA). 2-Fluoro-2-deoxyfucose was from CarboSynth (San Diego, CA). Dithiothreitol (DTT) was from Goldbio (St. Louis, MO). Cetyltrimethylammonium bromide, 5,5′-dithiobis-(2-nitrobenzoic acid) (DTNB), isopropyl β-D-1-thiogalactopyranoside (IPTG), 2-(*N*-morpholino)ethanesulfonic acid (MES), tris(hydroxymethyl)aminomethane (Tris), Tween X-100, bovine serum albumin (BSA), and other reagents, solvents, and buffers were from Sigma-Aldrich (St. Louis, MO) unless noted otherwise.

Glycan Synthesis. Globo H−biotin and Globo H−ceramide conjugates were synthesized from Globo H as described previously.[24,27,58] SSEA-4−biotin conjugate (Compound No. B295, Lot S284-1) was obtained from the Consortium for Functional Glycomics.

Peracetylated 2-Fluoro-2-deoxyfucose ($Ac_3$2FF). Peracetylated 2-fluoro-2-deoxyfucose was prepared from 2-fluoro-2-deoxyfucose by a procedure similar to that described previously.[43] Briefly, 2-fluoro-2-deoxyfucose (10.0 mg, 0.060 mmol) was dissolved in pyridine (0.35 mL), and the resulting solution was cooled to 0 °C. Acetic anhydride (0.020 mL, 0.22 mmol) was added, and the reaction vial was covered in foil and allowed to warm to room temperature overnight. The reaction mixture was then diluted with dichloromethane (5 mL) and washed with 1 M HCl (3 × 2 mL), saturated aqueous $NaHCO_3$ (3 mL), and brine (3 mL). The organics were dried over Na_2SO_4(s), concentrated under reduced pressure, and dried by high vacuum to provide peracetylated 2-fluoro-2-deoxyfucose in quantitative yield (17.5 mg; 0.060 mmol). NMR spectra were acquired on a Bruker spectrometer operating at 400 (^{1}H) and 101 (^{13}C) MHz and are shown in Figures S1 and S2. Chemical shift data are reported in units of δ (ppm) relative to residual solvent or TMS.

^{1}H NMR (400 MHz, $CDCl_3$, δ): α-anomer, 6.43 (d, J = 3.98 Hz, 1H, H-1), 5.42 (td, J = 10.64, 3.34 Hz, 1H, H-3), 5.37 (d, J = 3.70 Hz, 1H, H-4), 4.88 (ddd, J = 49.38, 10.17, 3.97 Hz, 1H, H-2), 4.25 (q, J = 6.53 Hz 1H, H-5), 2.18 (6H), 2.06 (s, 3H), 1.15 (d, J = 6.52 Hz, 3H, H-6); β-anomer, 5.77 (dd, J = 8.05, 4.12 Hz, 1H, H-1), 5.31 (s, 1H, H-4), 5.17 (ddd, J = 13.34, 9.89, 3.47 Hz, 1H, H-3), 4.64 (dt, J = 51.81, 8.90 Hz, 1H, H-2), 3.99 (q, J = 6.50 Hz, 1H, H-5), 2.23 (s, 3H), 2.18 (s, 3H), 2.06 (s, 3H), 1.22 (d, J = 6.44 Hz, 3H, H-6). ^{13}C NMR (101 MHz, $CDCl_3$, δ): α-anomer (major), δ 170.45, 170.23, 169.22, 89.34 (d, J = 21.62 Hz, C1), 84.36 (d, J = 190.72 Hz, C2), 71.19 (d, J = 7.49 Hz, C4), 68.73 (d, J = 19.1 Hz, C3), 67.26 (C5), 21.08, 20.82, 20.67, 15.88 (C6). HRMS (ESI): calcd for $C_{12}H_{17}FO_7$ $[M + NH_4]^+$ 310.1297; found, 310.1299.

Production of RNases. RNase A and RNase 1 were produced by heterologous expression of their cDNA in *Escherchia coli* strain BL21(DE3) and purification as described previously.[4] For conjugation of BODIPY, a cysteine residue was installed at residue 19 of the RNases with site-directed mutagenesis, and P19C RNase 1 and A19C RNase A were produced in a manner similar to that of the wild-type enzymes. After purification, the nascent thiol was protected as a mixed disulfide by reaction with DTNB. Prior to conjugation, the nascent thiol in 10 mg of protein was deprotected by the addition of DTT (4 equiv). The RNase was separated from excess DTT by passage through a column of PD-10 desalting resin from GE Healthcare (Pittsburgh, PA). The deprotected RNase was reacted with 10 equiv of BODIPY-Fl from Life Technologies dissolved in aqueous DMSO (10% v/v). The BODIPY-Fl solution was added dropwise with stirring, and the reaction was allowed to proceed at room temperature for 2 h, then at 4 °C for 4 h. After overnight dialysis into 50 mM AcOH, pH 5.0, purification by chromatography on a cation-exchange resin (GE Healthcare) yielded RNase−BODIPY conjugates. The identity of these conjugates was confirmed with matrix-assisted laser desorption/ionization (MALDI) mass spectroscopy at the University of Wisconsin Biotechnology Center and SDS−PAGE imaged by scanning for fluorescence and staining with Coomassie.

[^{15}N]-RNase A and [^{15}N]-RNase 1 were produced in *E. coli* as described previously,[4] except using a double-growth procedure in minimal medium containing [^{15}N]-NH_4Cl after induction with IPTG.[59] Growth conditions yielded an average of 15 mg of RNases from 1 L of medium. Protein purification was monitored with SDS−PAGE. The purified proteins were analyzed with MALDI mass spectroscopy. The observed masses of 14790.1 and 13809.2 Da indicated that isotope incorporation had been (13809−13681)/172 = 74% and (14790−14,604)/192 = 97% for RNase A and RNase 1, respectively.

Ribonucleolytic Activity Assays. RNases were assayed for catalytic activity by monitoring cleavage of a fluorogenic RNA substrate, 6-FAM−dArUdGdA−6-TAMRA from IDT (Coralville, IA).[60] Assays were performed in 0.10 M MES−NaOH [oligo(vinylsulfonic acid)-free[61]] buffer, pH 6.0, containing NaCl (0.10 M). The addition of RNases yielded a linear increase of fluorescence that can be converted into activity with the equation

DOI: 10.1021/acscentsci.5b00164
ACS Cent. Sci. 2015, 1, 181−190

$$k_{cat}/K_M = \frac{\Delta I/\Delta t}{(I_{max} - I_o)[\text{RNase}]} \quad (1)$$

where $\Delta I/\Delta t$ is the initial reaction velocity, I_{max} is the maximum detected fluorescence after saturating substrate with excess RNase A, and I_0 is the initial background fluorescence after incubation of substrate. The values of k_{cat}/K_M calculated with eq 1 were (31 ± 6) μM^{-1} s^{-1} and (2.1 ± 1.2) μM^{-1} s^{-1} for RNase A and RNase 1, respectively, and neither fluorescence labeling nor isotopic incorporation had a significant effect on these values.

Glycan Array Screening. A printed array of mammalian glycans was screened for RNase A ligands by the standard procedure of Core H of the Consortium for Functional Glycomics (CFG).[62] The array was version 2.0 and comprised 264 synthetic and natural glycans that are found on the surface of mammalian cells. The gycans were functionalized with an amino group and immobilized to *N*-hydroxysuccinimide-activated glass slides.[62]

Briefly, RNase A was diluted to a concentration of 200 μg/mL in 20 mM Tris−HCl buffer, pH 7.4, containing NaCl (150 mM), $CaCl_2$ (2 mM), $MgCl_2$ (2 mM), Tween 20 (0.05% v/v), and BSA (1% w/v). The binding of RNase A was detected by using α-RNase A (1 μg/mL) and a fluorescently labeled secondary antibody. The antibodies alone were also screened against the array, and the resulting fluorescence values were subtracted from values in the presence of RNase A.

Solid-Phase Glycan Binding Assay. Quantification of binding between RNases and immobilized glycans was monitored using a fluorescence surface-binding assay. Briefly, a 96-well plate coated in NeutrAvidin from Pierce (Rockford, IL) was washed with 3× PBS and then treated with 10 equiv of Globo H−biotin or SSEA-4−biotin. To reduce nonspecific interactions, wells were incubated with aqueous milk (5% v/v) and washed with PBS (3×). RNase−BODIPY conjugates were incubated to equilibrium in PBS, pH 7.4, containing Tween X-100 (0.005% v/v) or 20 mM Tris−HCl buffer, pH 5.0, containing NaCl (130 mM). After 3 washes, the fluorescence of an RNase−BODIPY conjugate was detected by emission at 530 nm after excitation at 490 nm. The fluorescence was corrected for that from a well treated with unconjugated biotin, and data were analyzed by nonlinear regression to the equation

$$B = \frac{B_{max}[\text{RNase}]^h}{K_d^{\,h} + [\text{RNase}]^h} \quad (2)$$

where B is the normalized relative fluorescence (RFU), B_{max} is the maximum percent fluorescence, and h is a Hill coefficient.

Cell Culture. Cells from the MCF-7 human breast adenocarcinoma line were grown in DMEM (high glucose) containing FBS (10% v/v) and pen/strep from Invitrogen. Cells were maintained at 37 °C in 5% CO_2.

Confocal Microscopy. Globo H on live cells was visualized with confocal microscopy. MCF-7 cells (1×10^5/well) in medium were grown for 3 days in the presence of $Ac_3$2FF (100 μM in 0.1% v/v DMSO)[43,44] or DMSO (0.1% v/v) alone. The medium was replaced with serum-free medium, and cells were plated in an 8-well microscopy slide from Ibidi (Verona, WI). The cell surface was stained with α-GH and a fluorescently labeled secondary antibody, or with WGA-488 from Life Technologies. Nuclei were stained with Hoechst 33342 from Life Technologies. Images were captured with an Eclipse TE2000-U laser-scanning confocal microscope from Nikon equipped with an Axio Camdigital camera from Carl Zeiss.

Flow Cytometry. Globo H on live cells was quantified with flow cytometry. MCF-7 cells (1×10^5/well) in medium were grown for 3 days in the presence of $Ac_3$2FF (100 μM in 0.1% v/v DMSO)[43,44] or DMSO (0.1% v/v) alone. The cells were incubated with α-GH and a fluorescently labeled secondary antibody. Fluorescence was measured with a FACSCalibur flow cytometer from BD Bioscience (San Jose, CA). Data were analyzed with FlowJo software from Tree Star (Ashland, OR).

Cell Viability Assay. The effect of Globo H on live cells was measured with an assay for cell viability. MCF-7 cells (5000/well) in medium were added to the wells of a 96-well plate from Corning (Corning, NY) and grown for 3 days in the presence of $Ac_3$2FF (100 μM in 0.1% v/v DMSO),[43,44] DMSO (0.1% v/v) alone, or H_2O_2 (1 mM). The medium was replaced with serum-free medium, and RNases in PBS were added at various concentrations. Cells were then incubated for 44 h. The medium was removed, and the cells were incubated in CellTiter 96 MTS reagent from Promega (Madison, WI) for 2 h. The absorbance was then measured at 490 nm and normalized to that from cells treated with 0.1% v/v DMSO alone (100%) and 1 mM H_2O_2 (0%).

Cellular DNA Synthesis Assay. The effect of Globo H on live cells was also measured with a sensitive assay for cellular DNA synthesis. MCF-7 cells (5000/well) in medium were added to the wells of a 96-well plate and grown overnight in medium. The medium was replaced with serum-free medium, and α-GH (final concentration: 15 ng/mL) was added to the wells. Then, DRRRD RNase 1 in PBS was added to the wells at three concentrations, and the cells were incubated for 44 h. Cell proliferation was assessed by monitoring the incorporation of [*methyl*-^{3}H]thymidine into cellular DNA, as described previously.[9]

Preparation of Samples for ^{1}H,^{15}N-HSQC NMR Spectroscopy. Samples were prepared in 600 μL with 100 mM KH_2PO_4 buffer, pH 6.5 or pH 4.7, containing [^{15}N]-RNase (250 μM), cetyltrimethylammonium bromide (25 mM), and D_2O (10% v/v). Globo H−ceramide conjugate was resuspended in $CHCl_3$/MeOH/H_2O 65:35:5. An aliquot containing 0.15 μmol of conjugate (1 equiv compared to the [^{15}N]-RNase) was dried under N_2(g) and then under high vacuum for 2 h. The conjugate was resuspended in the RNase-containing solution, which was then placed in an 8 in. glass tube from Wilmad-LabGlass (Vineland, NJ).

NMR data were recorded at 25 °C with a 600 MHz Varian NMR spectrometer. ^{1}H,^{15}N-HSQC NMR spectra were measured and peak assignments were made with the program Sparky 3 (T. D. Goddard and D. G. Kneller, University of California, San Francisco) using the assignments determined from the solution structures of RNase 1[63] and RNase A.[59] The vector change of chemical shift ($\Delta\Delta\delta$) upon addition of the Globo H−ceramide conjugate (1 equiv) was determined with the equation

$$\Delta\Delta\delta = \sqrt{(\Delta\delta^1\text{H})^2 + \left(\frac{1}{5}\Delta\delta^{15}\text{N}\right)^2} \quad (3)$$

where ^{1}H and ^{15}N chemical shifts ($\Delta\delta$) were determined by subtracting the peak chemical shifts of RNase in the absence of the Globo H−ceramide conjugate. To depict the chemical shift perturbations, images of PDB entry 2k11[63] were created with

DOI: 10.1021/acscentsci.5b00164
ACS Cent. Sci. 2015, 1, 181−190

the program PyMOL from Schrödinger (New York, NY) in which values of $\Delta\Delta\delta$ were inserted as the β-factor.

■ ASSOCIATED CONTENT

Supporting Information

The following file is available free of charge on the ACS Publications website at DOI: 10.1021/acscentsci.5b00164.

Identity of the 264 glycans in the glycan array, spectral characterization of peracetylated 2-fluoro-2-deoxyfucose, raw $^{1}H,^{15}N$-HSQC NMR spectra, and chemical shift perturbations of RNase A in the presence of Globo H−ceramide micelles at pH 4.7 (PDF)

■ AUTHOR INFORMATION

Corresponding Author

*E-mail: rtraines@wisc.edu.

Notes

The authors declare the following competing financial interest(s): R.T.R. is a founder of Quintessence Biosciences, Inc. (Madison, WI), which is developing cancer chemotherapeutic agents based on ribonucleases.

■ ACKNOWLEDGMENTS

We are grateful to Dr. M. R. Levengood (Seattle Genetics) for suggesting the use of peracetylated 2-fluoro-2-deoxyfucose and to M. R. Aronoff (University of Wisconsin Madison) for its synthesis, and to Drs. W. M. Westler and M. Tonelli (University of Wisconsin Madison) for advice with HSQC NMR spectroscopy. We thank Prof. C. J. Czuprynski (University of Wisconsin Madison) for providing transformed (MAC-T) bovine mammary gland epithelial cells. This work was supported by Grant R01 CA073808 (NIH). The glycan array screen and SSEA-4 biotin were provided by the Consortium for Functional Glycomics, which was supported by Grant U54 GM062116 (NIH). This study made use of the Organic Synthesis Core Facility at the Memorial Sloan Kettering Cancer Center, which was supported by Grant P30 CA008748 (NIH), and the National Magnetic Resonance Facility at Madison, which was supported by Grant P41 GM103399 (NIH). T.-Y.C. was supported by the Dr. James Chieh-Hsia Mao Wisconsin Distinguished Graduate Fellowship.

■ REFERENCES

(1) Raines, R. T. Ribonuclease A. *Chem. Rev.* **1998**, *98*, 1045−1066.

(2) Eller, C. H.; Lomax, J. E.; Raines, R. T. Bovine brain ribonuclease is the functional homolog of human ribonuclease 1. *J. Biol. Chem.* **2014**, *289*, 25996−26006.

(3) Dickson, K. A.; Haigis, M. C.; Raines, R. T. Ribonuclease inhibitor: Structure and function. *Prog. Nucleic Acid Res. Mol. Biol.* **2005**, *80*, 349−374.

(4) Leland, P. A.; Schultz, L. W.; Kim, B.-M.; Raines, R. T. Ribonuclease A variants with potent cytotoxic activity. *Proc. Natl. Acad. Sci. U.S.A.* **1998**, *95*, 10407−10412.

(5) Leland, P. A.; Staniszewski, K. E.; Kim, B.-M.; Raines, R. T. Endowing human pancreatic ribonuclease with toxicity for cancer cells. *J. Biol. Chem.* **2001**, *276*, 43095−43102.

(6) Rutkoski, T. J.; Kurten, E. L.; Mitchell, J. C.; Raines, R. T. Disruption of shape-complementarity markers to create cytotoxic variants of ribonuclease A. *J. Mol. Biol.* **2005**, *354*, 41−54.

(7) Johnson, R. J.; McCoy, J. G.; Bingman, C. A.; Phillips, G. N., Jr.; Raines, R. T. Inhibition of human pancreatic ribonuclease by the human ribonuclease inhibitor protein. *J. Mol. Biol.* **2007**, *367*, 434−449.

(8) Rutkoski, T. J.; Raines, R. T. Evasion of ribonuclease inhibitor as a determinant of ribonuclease cytotoxicity. *Curr. Pharm. Biotechnol.* **2008**, *9*, 185−199.

(9) Lomax, J. E.; Eller, C. H.; Raines, R. T. Rational design and evaluation of mammalian ribonuclease cytotoxins. *Methods Enzymol.* **2012**, *502*, 273−290.

(10) ClinicalTrials.gov Identifier: NCT00818831.

(11) Haigis, M. C.; Kurten, E. L.; Raines, R. T. Ribonuclease inhibitor as an intracellular sentry. *Nucleic Acids Res.* **2003**, *31*, 1024−1032.

(12) Dube, D. H.; Bertozzi, C. R. Glycans in cancer and inflammation—potential for therapeutics and diagnostics. *Nat. Rev. Drug Discovery* **2005**, *4*, 477−488.

(13) Levine, M. N.; Hoang, T. T.; Raines, R. T. Fluorogenic probe for constitutive cellular endocytosis. *Chem. Biol.* **2013**, *20*, 614−618.

(14) Sundlass, N. K.; Eller, C. H.; Cui, Q.; Raines, R. T. Contribution of electrostatics to the binding of pancreatic-type ribonucleases to membranes. *Biochemistry* **2013**, *52*, 6304−6312.

(15) Johnson, R. J.; Chao, T.-Y.; Lavis, L. D.; Raines, R. T. Cytotoxic ribonucleases: The dichotomy of Coulombic forces. *Biochemistry* **2007**, *46*, 10308−10316.

(16) Chao, T.-Y.; Lavis, L. D.; Raines, R. T. Cellular uptake of ribonuclease A relies on anionic glycans. *Biochemistry* **2010**, *49*, 10666−10673.

(17) Varki, A. P.; Baum, L. G.; Bellis, S. L.; Cummings, R. D.; Esko, J. D.; Hart, G. W.; Linhardt, R. J.; Lowe, J. B.; McEver, R. P.; Srivastava, A.; Sarkar, R. Working group report: The roles of glycans in hemostasis, inflammation and vascular biology. *Glycobiology* **2008**, *18*, 747−749.

(18) Drickamer, K.; Taylor, M. E. Glycan arrays for functional glycomics. *Genome Biol.* **2002**, *3*, 1034.

(19) Mariani-Costantini, R.; Barbanti, P.; Colnaghi, M. I.; Menard, S.; Clemente, C.; Rilke, F. Reactivity of a monoclonal antibody with tissues and tumors from the human breast. Immunohistochemical localization of a new antigen and clinicopathologic correlations. *Am. J. Pathol.* **1984**, *115*, 47−56.

(20) Mariani-Costantini, R.; Colnaghi, M. I.; Leoni, F.; Menard, S.; Cerasoli, S.; Rilke, F. Immunohistochemical reactivity of a monoclonal antibody prepared against human breast carcinoma. *Virchows Archiv. A: Pathol. Anat. Histopathol.* **1984**, *402*, 389−404.

(21) Zhang, S.; Cordon-Cardo, C.; Zhang, H. S.; Reuter, V. E.; Adluri, S.; Hamilton, W. B.; Lloyd, K. O.; Livingston, P. O. Selection of tumor antigens as targets for immune attack using immunohistochemistry: I. Focus on gangliosides. *Int. J. Cancer* **1997**, *73*, 42−49.

(22) Martignone, S.; Menard, S.; Bedini, A.; Paccagnella, A.; Fasolato, S.; Veggian, R.; Colnaghi, M. I. Study of the expression and function of the tumour-associated antigen CaMBr1 in small cell lung carcinomas. *Eur. J. Cancer* **1993**, *29A*, 2020−2025.

(23) Perrone, F.; Menard, S.; Canevari, S.; Calabrese, M.; Boracchi, P.; Bufalino, R.; Testori, S.; Baldini, M.; Colnaghi, M. I. Prognostic significance of the CaMBr1 antigen on breast carcinoma: Relevance of the type of recognised glycoconjugate. *Eur. J. Cancer* **1993**, *29A*, 2113−2117.

(24) Tsai, Y.-C.; Huang, J.-R.; Cheng, J.-Y.; Lin, J.-J.; Hung, J.-T.; Wu, Y.-Y.; Yeh, K.-T.; Yu, A. L. A prevalent cancer associated glycan, Globo H ceramide, induces immunosuppression by reducing Notch1 signaling. *J. Cancer Sci. Ther.* **2013**, *5*, 264−270.

(25) Cheng, J.-Y.; Wang, S.-H.; Lin, J.; Tsai, Y.-C.; Yu, J.; Wu, J.-C.; Hung, J.-T.; Lin, J.-J.; Wu, Y.-Y.; Yeh, K.-T.; Yu, A. L. Globo-H ceramide shed from cancer cells triggers translin-associated factor X−dependent angiogenesis. *Cancer Res.* **2014**, *74*, 6856−6866.

(26) Danishefsky, S. J.; Shue, Y.-K.; Chang, M. N.; Wong, C.-H. Development of Globo-H cancer vaccine. *Acc. Chem. Res.* **2015**, *48*, 643−652.

(27) Eller, C. H.; Yang, G.; Ouerfelli, O.; Raines, R. T. Affinity of monoclonal antibodies to globo-series glycans. *Carbohydr. Res.* **2014**, *397*, 1−6.

DOI: 10.1021/acscentsci.5b00164
ACS Cent. Sci. 2015, 1, 181−190

(28) Cascinelli, N.; Doci, R.; Belli, F.; Nava, M.; Marolda, R.; Costa, A.; Menard, S.; Terno, G. Evaluation of toxic effects following administration of monoclonal antibody MBr1 in patients with breast cancer. *Tumori* **1986**, *72*, 267−271.
(29) Kim, I. J.; Park, T. K.; Hu, S. H.; Abrampah, K.; Zhang, S. L.; Livingston, P. O.; Danishefsky, S. J. Defining the molecular recognition of Globo-H (human breast-cancer) antigen through probe structures prepared by total synthesis. *J. Org. Chem.* **1995**, *60*, 7716−7717.
(30) Bilodeau, M. T.; Park, T. K.; Hu, S.; Randolph, J. T.; Danishefsky, S. J.; Livingston, P. O.; Zhang, S. Total synthesis of a human breast tumor associated antigen. *J. Am. Chem. Soc.* **1995**, *117*, 7840−7841.
(31) Ouerfelli, O.; Warren, J. D.; Wilson, R. M.; Danishefsky, S. J. Synthetic carbohydrate-based antitumor vaccines: Challenges and opportunities. *Expert Rev. Vaccines* **2005**, *4*, 677−685.
(32) Zhu, J.; Wan, Q.; Lee, D.; Yang, G.; Spassova, M. K.; Ouerfelli, O.; Ragupathi, G.; Damani, P.; Livingston, P. O.; Danishefsky, S. J. From synthesis to biologics: Preclinical data on a chemistry derived anticancer vaccine. *J. Am. Chem. Soc.* **2009**, *131*, 9298−9303.
(33) ClinicalTrials.gov Identifiers: NCT01248273 and NCT01349647.
(34) Endo, M.; Suzuki, K.; Schmid, K.; Fournet, B.; Karamanos, Y.; Montreuil, J.; Dorland, L.; van Halbeek, H.; Vliegenthart, J. F. The structures and microheterogeneity of the carbohydrate chains of human plasma ceruloplasmin. A study employing 500-MHz ^{1}H-NMR spectroscopy. *J. Biol. Chem.* **1982**, *257*, 8755−8760.
(35) Charlwood, J.; Birrell, H.; Tolson, D.; Camilleri, P. Two-dimensional chromatography in the analysis of complex glycans from transferrin. *Anal. Chem.* **1998**, *70*, 2530−2535.
(36) Nakano, M.; Kakehi, K.; Tsai, M. H.; Lee, Y. C. Detailed structural features of glycan chains derived from α_1-acid glycoproteins of several different animals: The presence of hypersialylated, *O*-acetylated sialic acids but not disialyl residues. *Glycobiology* **2004**, *14*, 431−441.
(37) Chester, M. A. Nomenclature of glycolipids. *Pure Appl. Chem.* **1997**, *69*, 2475−2487.
(38) D'Angelo, G.; Capasso, S.; Sticco, L.; Russo, D. Glycosphingolipids: Synthesis and functions. *FEBS J.* **2013**, *280*, 6338−6353.
(39) Kannagi, R.; Cochran, N. A.; Ishigami, F.; Hakomori, S.; Andrews, P. W.; Knowles, B. B.; Solter, D. Stage-specific embryonic antigens (SSEA-3 and −4) are epitopes of a unique globo-series ganglioside isolated from human teratocarcinoma cells. *EMBO J.* **1983**, *2*, 2355−2361.
(40) Venable, A.; Mitalipova, M.; Lyons, I.; Jones, K.; Shin, S.; Pierce, M.; Stice, S. Lectin binding profiles of SSEA-4 enriched, pluripotent human embryonic stem cell surfaces. *BMC Dev. Biol.* **2005**, *5*, 15.
(41) Adobati, E.; Zacchetti, A.; Perico, M. E.; Cremonesi, F.; Rasi, G.; Vallebona, P. S.; Hagenaars, M.; Kuppen, P. J.; Pastan, I.; Panza, L.; Russo, G.; Colnaghi, M. I.; Canevari, S. Expression profile of saccharide epitope CaMBr1 in normal and neoplastic tissue from dogs, cats, and rats: Implication for the development of human-derived cancer vaccines. *Histochem. J.* **1999**, *31*, 729−737.
(42) Huynh, H. T.; Robitaille, G.; Turner, J. D. Establishment of bovine mammary epithelial cells (MAC-T): An *in vitro* model for bovine lactation. *Exp. Cell Res.* **1991**, *197*, 191−199.
(43) Rillahan, C. D.; Antonopoulos, A.; Lefort, C. T.; Sonon, R.; Azadi, P.; Ley, K.; Dell, A.; Haslam, S. M.; Paulson, J. C. Global metabolic inhibitors of sialyl- and fucosyltransferases remodel the glycome. *Nat. Chem. Biol.* **2012**, *8*, 661−668.
(44) Okeley, N. M.; Alley, S. C.; Anderson, M. E.; Boursalian, T. E.; Burke, P. J.; Emmerton, K. M.; Jeffrey, S. C.; Klussman, K.; Law, C. L.; Sussman, D.; Toki, B. E.; Westendorf, L.; Zeng, W. P.; Zhang, X. Q.; Benjamin, D. R.; Senter, P. D. Development of orally active inhibitors of protein and cellular fucosylation. *Proc. Natl. Acad. Sci. U.S.A.* **2013**, *110*, 5404−5409.
(45) van Meer, G.; Voelker, D. R.; Feigenson, G. W. Membrane lipids: Where they are and how they behave. *Nat. Rev. Mol. Cell Biol.* **2008**, *9*, 112−124.
(46) Tycko, B.; Maxfield, F. R. Rapid acidification of endocytic vesicles containing α_2-macroglobulin. *Cell* **1982**, *28*, 643−651.
(47) Yamashiro, D. J.; Tycko, B.; Fluss, S. R.; Maxfield, F. R. Segregation of transferrin to a mildly acidic (pH 6.5) para-Golgi compartment in the recycling pathway. *Cell* **1984**, *37*, 789−800.
(48) Fischer, S.; Nishio, M.; Dadkhahi, S.; Gansler, J.; Saffarzadeh, M.; Shibamiyama, A.; Kral, N.; Baal, N.; Koyama, T.; Deindl, E.; Preissner, K. T. Expression and localisation of vascular ribonucleases in endothelial cells. *Thromb. Haemostasis* **2011**, *105*, 345−355.
(49) Chao, T.-Y.; Raines, R. T. Mechanism of ribonuclease A endocytosis: Analogies to cell-penetrating peptides. *Biochemistry* **2011**, *50*, 8374−8382.
(50) Toyama, Y.; Ueyama, J.; Nomura, H.; Tsukiyama, I.; Saito, H.; Hisada, T.; Matsuura, K.; Hasegawa, T. Contribution of plasma proteins, albumin and α_1-acid glycoprotein, to pharmacokinetics of a multi-targeted receptor tyrosine kinase inhibitor, sunitinib, in analbuminemic rats. *Anticancer Res.* **2014**, *34*, 2283−2289.
(51) Rutkoski, T. J.; Kink, J. A.; Strong, L. E.; Raines, R. T. Site-specific PEGylation endows a mammalian ribonuclease with antitumor activity. *Cancer Biol. Ther.* **2011**, *12*, 208−214.
(52) Rutkoski, T. J.; Kink, J. A.; Strong, L. E.; Raines, R. T. Human ribonuclease with a pendant poly(ethylene glycol) inhibits tumor growth in mice. *Transl. Oncol.* **2013**, *6*, 392−397.
(53) Findlay, D.; Herries, D. G.; Mathias, A. P.; Rabin, B. R.; Ross, C. A. The active site and mechanism of action of bovine pancreatic ribonuclease. *Nature* **1961**, *190*, 781−784.
(54) Cuchillo, C. M.; Nogués, M. V.; Raines, R. T. Bovine pancreatic ribonuclease: Fifty years of the first enzymatic reaction mechanism. *Biochemistry* **2011**, *50*, 7835−7841.
(55) Anfinsen, C. B. Principles that govern the folding of protein chains. *Science* **1973**, *181*, 223−230.
(56) Moore, S.; Stein, W. H. Chemical structures of pancreatic ribonuclease and deoxyribonuclease. *Science* **1973**, *180*, 458−464.
(57) Merrifield, R. B. Solid phase synthesis. *Science* **1984**, *232*, 341−347.
(58) Jeon, I.; Iyer, K.; Danishefsky, S. J. A practical total synthesis of Globo-H for use in anticancer vaccines. *J. Org. Chem.* **2009**, *74*, 8452−8455.
(59) Tonelli, M.; Eller, C. H.; Singarapu, K. K.; Lee, W.; Bahrami, A.; Westler, W. M.; Raines, R. T.; Markley, J. L. Assignments of RNase A by ADAPT-NMR and enhancer. *Biomol. NMR Assignments* **2015**, *9*, 81−88.
(60) Kelemen, B. R.; Klink, T. A.; Behlke, M. A.; Eubanks, S. R.; Leland, P. A.; Raines, R. T. Hypersensitive substrate for ribonucleases. *Nucleic Acids Res.* **1999**, *27*, 3696−3701.
(61) Smith, B. D.; Soellner, M. B.; Raines, R. T. Potent inhibition of ribonuclease A by oligo(vinylsulfonic acid). *J. Biol. Chem.* **2003**, *278*, 20934−20938.
(62) Blixt, O.; Head, S.; Mondala, T.; Scanlan, C.; Huflejt, M. E.; Alvarez, R.; Bryan, M. C.; Fazio, F.; Calarese, D.; Stevens, J.; Razi, N.; Stevens, D. J.; Skehel, J. J.; van Die, I.; Burton, D. R.; Wilson, I. A.; Cummings, R.; Bovin, N.; Wong, C.-H.; Paulson, J. C. Printed covalent glycan array for ligand profiling of diverse glycan binding proteins. *Proc. Natl. Acad. Sci. U.S.A.* **2004**, *101*, 17033−17038.
(63) Köver, K. E.; Bruix, M.; Santoro, J.; Batta, G.; Laurents, D. V.; Rico, M. The solution structure and dynamics of human pancreatic ribonuclease determined by NMR spectroscopy provide insight into its remarkable biological activities and inhibition. *J. Mol. Biol.* **2008**, *379*, 953−965.

DOI: 10.1021/acscentsci.5b00164
ACS Cent. Sci. 2015, 1, 181−190